Investigating the Effectiveness of Vortex Generators in Aviation through High-Fidelity CFD Analysis

Mihai-Vladut HOTHAZIE*,[1,2], Ionut BUNESCU[1,2], Mihaita-Gilbert STOICAN[1,2], Dennis-Stefan CHELEMEN[1,2]

*Corresponding author
[1]INCAS – National Institute for Aerospace Research "Elie Carafoli", B-dul Iuliu Maniu 220, 061126, Bucharest, Romania,
hothazie.mihai@incas.ro*, bunescu.ionut@incas.ro, stoican.gilbert@incas.ro, chelemen.stefan@incas.ro
[2]"POLITEHNICA" University of Bucharest, Faculty of Aerospace Engineering, Str. Gheorghe Polizu 1-7, 011061, Bucharest, Romania

DOI: 10.13111/2066-8201.2024.16.3.5

Received: 03 July 2024/ Accepted: 08 August 2024/ Published: September 2024

Abstract: *The present study highlights the benefits of using vortex generators as a passive boundary layer control method to delay the flow separation. Using high fidelity CFD analysis, a parametric study regarding the optimum position of vortex generators is carried out using an in-house automation procedure. After that, relevant quantities such as wall shear stress, turbulent kinetic energy, pressure coefficient distribution and oil flow visualization are analyzed and corresponding conclusions are drawn. The use of turbulent and energy quantities allows to quantify the impact of the generated vortices on the boundary layer and to identify the optimal positioning of vortex generators for improved aerodynamic performance.*

Key Words: *vortex generators, CFD, oil flow visualization, automation process, parametric study, turbulent kinetic energy*

1. INTRODUCTION

Originating from Prandtl's manuscript on boundary-layer theory, methods for delaying the transition or separation point of the flow have been extensively studied in the aerospace industry. The complexity of the turbulent flow problem greatly increased the effort of understanding and creating boundary layer control devices used to effect beneficial changes in the wall-bounded region. Such methods can be grouped into passive or active flow control devices. The main advantage of being non-energy consumptive is of the former, while versatility and superior performance are the advantages of the latter. The overall benefit of using these devices usually includes an overall drag reduction and lift enhancement, whatever the purpose: delay or advance the transition point, suppress, or enhance the turbulence either prevent or induce the flow separation. Studies have shown that energy losses together with the deficit of momentum in the boundary layer region are clear indications of possible flow separation [1]. To overcome the adverse pressure gradient, additional energy from the exterior part of the flow or from another source of energy must be added in the flow. In [2], [3], a comparison of different types of control methods was presented, and the use of passive vortex generators has been found to be the most effective for improving the aerodynamic performance of the blades. In addition, simplicity and robustness led to a high rate of adoption in the commercial sector. The downstream concentrated vortices developed by the vortex generators transport the high energy fluid outside the boundary layer into the near wall region enhancing the mixing process and thickening the boundary layer velocity profile by increasing the kinetic energy of the fluid [4], [5]. Even though numerous studies have been conducted and different performance criteria have been concluded such as the dimension of the vortex scale or vortex core spacing [6], the circulation and peak-vorticity [7] or geometrical parameters [8], [9] a general performance criterion widely utilized by research scientists has not been defined. In [10], using three-dimensional particle image velocimetry, wind tunnel testing was performed and showed that vortex generators transfer momentum from the outer flow into the boundary layer and as the flow advances, the mixing process increases.

However, accurately predicting the behavior of vortex generators using CFD simulations poses computational challenges. The grid size problem arises due to the requirement of fine resolution near the vortex generators to accurately capture small-scale flow phenomena. This leads to an increase in computational effort and time, limiting the feasibility of parametric studies and design optimization. To address these challenges, a 2.5D grid approach coupled with polyhedral meshing techniques was used. This approach reduces the computational effort while still capturing the essential three-dimensional effects near the vortex generators [11]. Additionally, we leverage the advantages of polyhedral meshing, which offers improved efficiency and accuracy compared to traditional meshing methods [12]. The polyhedral meshing technique enables a more accurate representation of complex geometries with fewer computational elements. By employing this meshing approach, we aim to reduce the overall mesh size and subsequently decrease the computational effort required for the parametric study of vortex generator positioning.

This paper focuses on analyzing the flow physics around the vortex generators and the importance of position in the overall efficiency of the control method. In the following, an outline of the methodology that we have used is presented together with representative quantities such as wall shear stress or turbulent kinetic energy. In addition, an automation process involving the domain and grid generation as well as the aerodynamic performance analysis using a high-fidelity CFD solver to assist the parametric study is presented together with the overall corresponding conclusions.

2. METHODOLOGY

The complexity of the downstream turbulent flow generated by the vortex generator can be properly studied with the help of numerical simulation. The aim of this paper is to determine additional performance criteria for defining the efficiency of the vortex generators by comparing the differences between the induced flow field characteristics of different positionings in a parametric driven study. The numerical simulations were performed using commercial CFD code, Ansys Fluent, while the computational grid was generated using Fluent Meshing. The computational domain was generated similarly to other previous studies such as [13], [14] to minimize computational effort and includes a wing section with NACA 63-618 airfoil at $Re = 2 \cdot 10^6$. Figure 1 the defining geometrical parameters of the domain where R=25c and b represents the span of the domain. The vortex generators were chosen to be conventional counter clockwise triangular shape with $h = 0.01m$, $l = 0.02m$, $\delta = 0.001m$, $\beta = 24^o$ similar to the ones used in [8]. The domain was chosen such that a single pair of vortex generators is modelled and periodic conditions are applied on the lateral sides of the domain and replicates the distance between two pairs of generators, λ as the wing span b. This helps to minimize the computational grid size and avoids the wing tip effect.

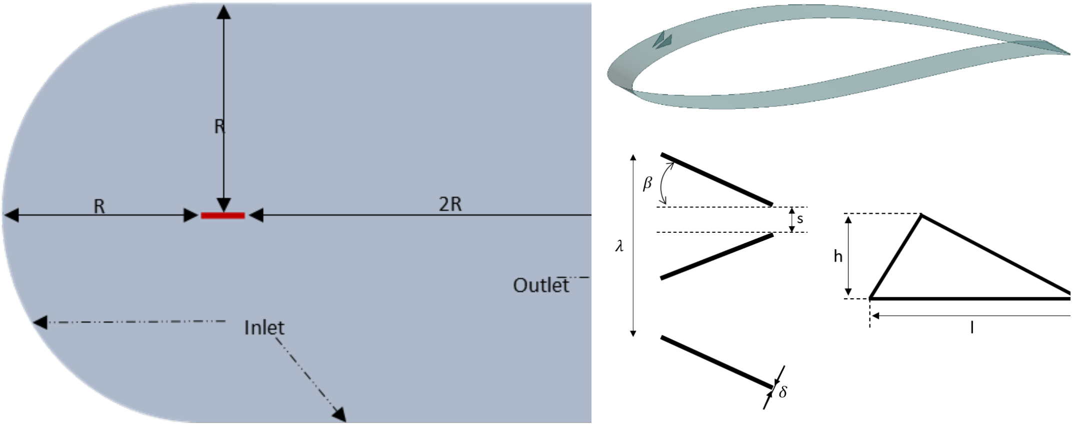

Figure 1. Computational domain and vortex generators geometry parameters.

The polyhedral cell type was chosen for the grid generation in Fluent Meshing and adapted with near-wall mesh height corresponding to $y^+ = 1$ with a global ratio of 1.1. The boundary layer region was generated using prismatic layers with a first cell height of $2.5 \cdot 10^{-5} m$ and a number of 35 layers. To properly capture the specific turbulent structures correlated to the vortex generators, a minimum of 10 cells on the thickness of the generator was imposed. Non-conform periodic boundary conditions were imposed on the lateral sides of the domain while on inlet, a velocity-inlet boundary condition was used. The pressure outlet condition defined the outflow region of the domain and a no slip condition was applied on the surface of the wing.

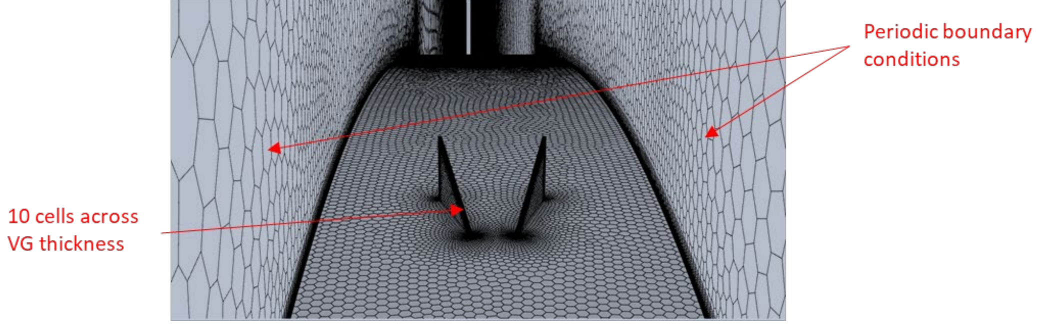

Figure 2. Polyhedral grid and boundary conditions

The polyhedral cells were chosen for the combined benefits of hexahedral cells which have a low numerical diffusion which contributes to the accuracy of the solution, and the versatility of tetrahedral cells for easily and accurately capturing complex geometries. In addition, another benefit of polyhedral cells is the high number of neighboring cells which contribute to a better approximation of the numerical gradients [11]. The numerical solution was obtained using a widely used commercial solver, Fluent, where RANS (Reynolds-averaged Navier-Stokes equations) were solved for a steady-state flow using the SIMPLE (Semi-Implicit-Pressure-Linked-Equations) algorithm.

For the parametric study, an automation process was developed to minimize the computational time required and minimize the human interaction. For this, commercial programs such as Workbench, Design Modeler, Fluent Meshing and Fluent solver were linked together with the help of MATLAB. Starting from a MATLAB script, with the help of a Windows batch file, Workbench is started. Using a python script, Workbench is used to start the domain generation tool (Design Modeler). With the help of a Jscript, the computational domain is generated and exported to Fluent meshing where using a predefined journal the computational grid is obtained and exported to Fluent solver. After the numerical solution is obtained, using MATLAB, the aerodynamic performances are read. In Figure 3, a logical scheme of the process is presented.

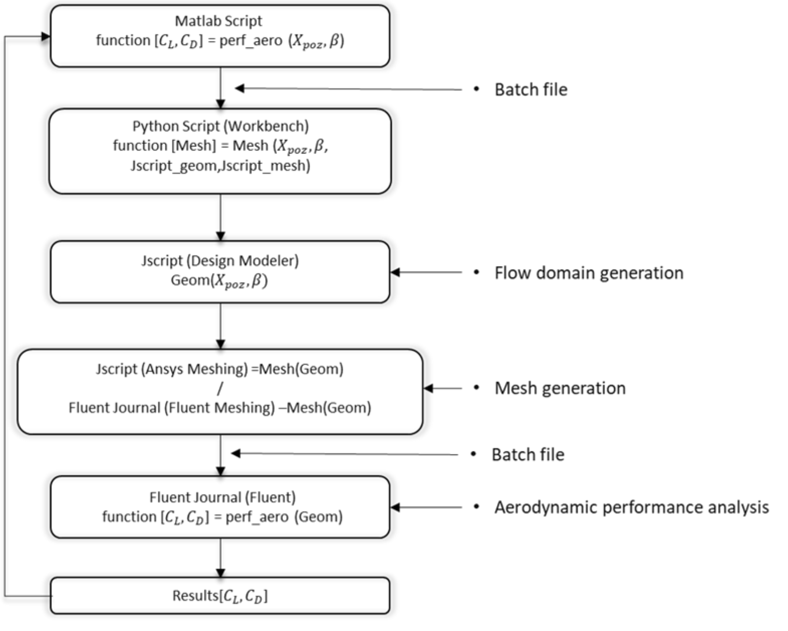

Figure 3. Logical schema of the automation process

3. RESULTS

Although other geometrical parameters were studied, significant results were obtained for the chordwise vortex generator position relative to the leading edge of the wing section. In the following, results will be presented for four significant positions (0.1c,0.2c,0.3c,0.4c) as shown in the table below.

Table 1: Cases Studied

	Case 0	**Case 1**	**Case 2**	**Case 3**	**Case 4**
Position	w\o VGS	0.1c VGS	0.2c VGS	0.3c VGS	0.4c VGS

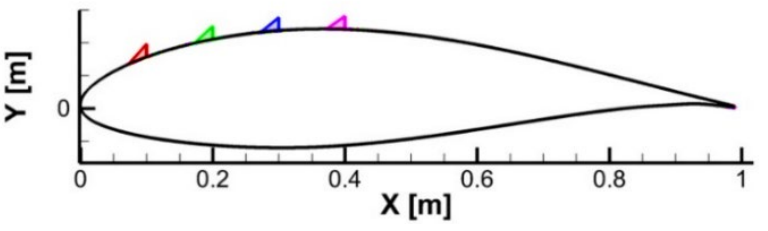

Figure 4. Vortex generators positions for every case

Figure 5 shows the numerical solution obtained for different chordwise position of the vortex generators in comparison to the clean wing section. The lift curve underlines the effectiveness of the vortex generators relative to the clean configuration. Positioning the vortex generators further downstream leads to a decrease in the stall angle from 23^0 at 0.1c to 15^0 at 0.4c and shows that a proper positioning can lead to an increase by 23% in the lift coefficient and an increase of 9^0 in the stall angle compared to the baseline case. Although significant increases in maximum lift coefficient and stall angle are shown, an overall perspective on the results show that the post stall lift slope is inversely proportional to the positioning of the vortex generators. This shows that the chordwise position of the generators does have an important role for the post stall performance and a sudden decrease in lift coefficient must be avoided for safety reasons. While, there is no variation of the lift slope between different configurations, a performance criterion such as the value of the stall angle can be used in an optimization procedure. Drag variation with angle of attack is shown below and shows a significant reduction of drag coefficient after the base line stall angle for every vortex generator configuration that we have studied.

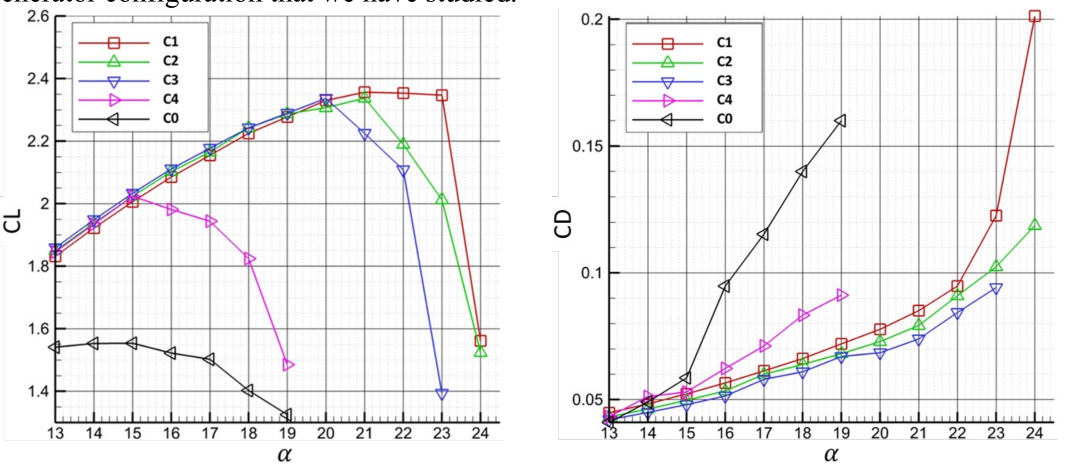

(a) (b)

Figure 5. Lift and drag polars

The distribution of the pressure coefficient in the middle section for every case at $\alpha = 22^0$ is shown in Figure 6. A decrease in the pressure coefficient on the upper surface can be seen near the vortex generators for every position except the $0.4c$ positioning.

The increase in lift is partly attributed to the acceleration of the fluid between the generators due to the vortex tubes that are being created, and partly due to the fluid suction effect which occurs before the generators. The $0.4c$ positioning shows no lift increase due to the lack of the mixing process created by the vortex tubes and denotes a lack vortex generator efficiency.

The distribution of the pressure coefficient in the middle section for every case at $\alpha = 22^0$ is shown in Figure 6. A decrease in the pressure coefficient on the upper surface can be seen near the vortex generators for every position except the $0.4c$ positioning.

The increase in lift is partly attributed to the acceleration of the fluid between the generators due to the vortex tubes that are being created, and partly due to the fluid suction effect which occurs before the generators. The $0.4c$ positioning shows no lift increase due to the lack of the mixing process created by the vortex tubes and denotes a lack vortex generator efficiency.

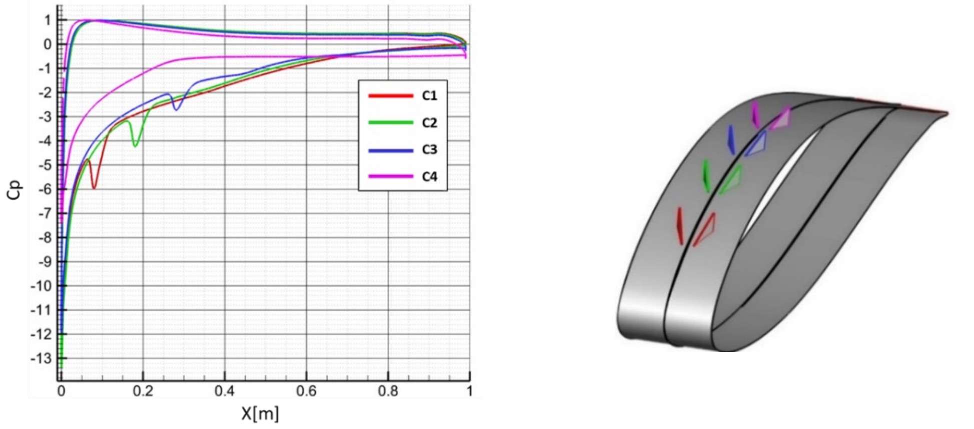

(a) (b)

Figure 6. Pressure coefficient distribution for the middle section for all configuration at $\alpha = 22^o$

In Figure 7 flow separation zones, which are associated with low energy dissipation in the boundary layer region, are shown for all configurations at$\alpha = 22^0$. The position of the vortex generators near the leading edge increases the efficiency of the control method by reducing the surface area of the flow separation zones. The 0.4c positioning shows the occurrence of flow separation before the vortex generators and does not have significant impact on controlling the flow. Notably, separation tends to occur only on the lateral sides of the wing section which indicates the beneficial influence of the downstream generated vortex tubes. The overlap of the separation lines shows a dependency of the separation area to the positioning of the vortex generators.

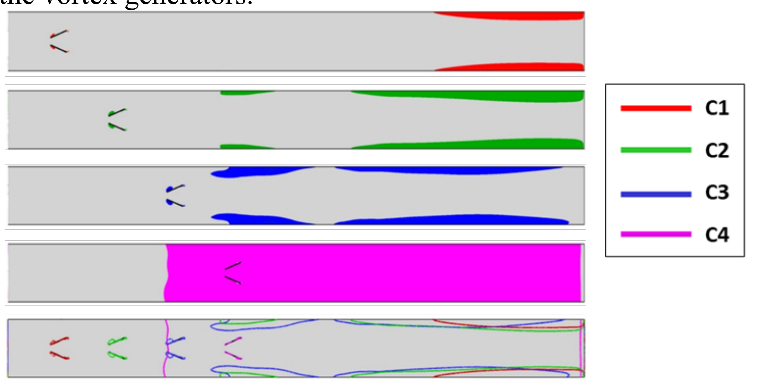

Figure 7. Representation of flow separation zones

In Figure 8, a comparison between velocities contours plotted on equidistant planes perpendicular to the vortex generators surfaces for the three configurations at $\alpha = 22^0$ is presented. The region near the top of the vortex generator indicates a recirculation zone. Moreover, the area of the recirculation zone shown with the help of the downstream perpendicular planes increases and indicates that the vortex tubes are generated from the vortex generator surface. A comparison between the three positions shows a dependency between the efficiency of the vortex generator and the size of the recirculation zone. This behaviour can be explained by the pressure difference connecting the exterior and interior surface of the generator. Positioning the vortex generators at $0.1c$, the recirculation zone occurs at about 60% of the vortex generator length, whereas positioning at $0.3c$, the recirculation zone starts at about 20%. This implies that another performance criteria that can be used for validation only is the size of the recirculation zone.

The same comparison was done in terms of the turbulent kinetic energy and shows that the recirculation zone has highly turbulent flow. As the efficiency of the vortex generators is decreased by positioning further downstream, the overall turbulent kinetic energy decreases. In the case of $0.1c$ positioning, the creation of the vortex tubes from the front of the vortex generator can be seen. Additionally, a correlation between the turbulent kinetic energy and velocity contours can be concluded. A high turbulent kinetic energy zone corresponds to an area of small recirculation zone which leads to a highly efficient vortex tube.

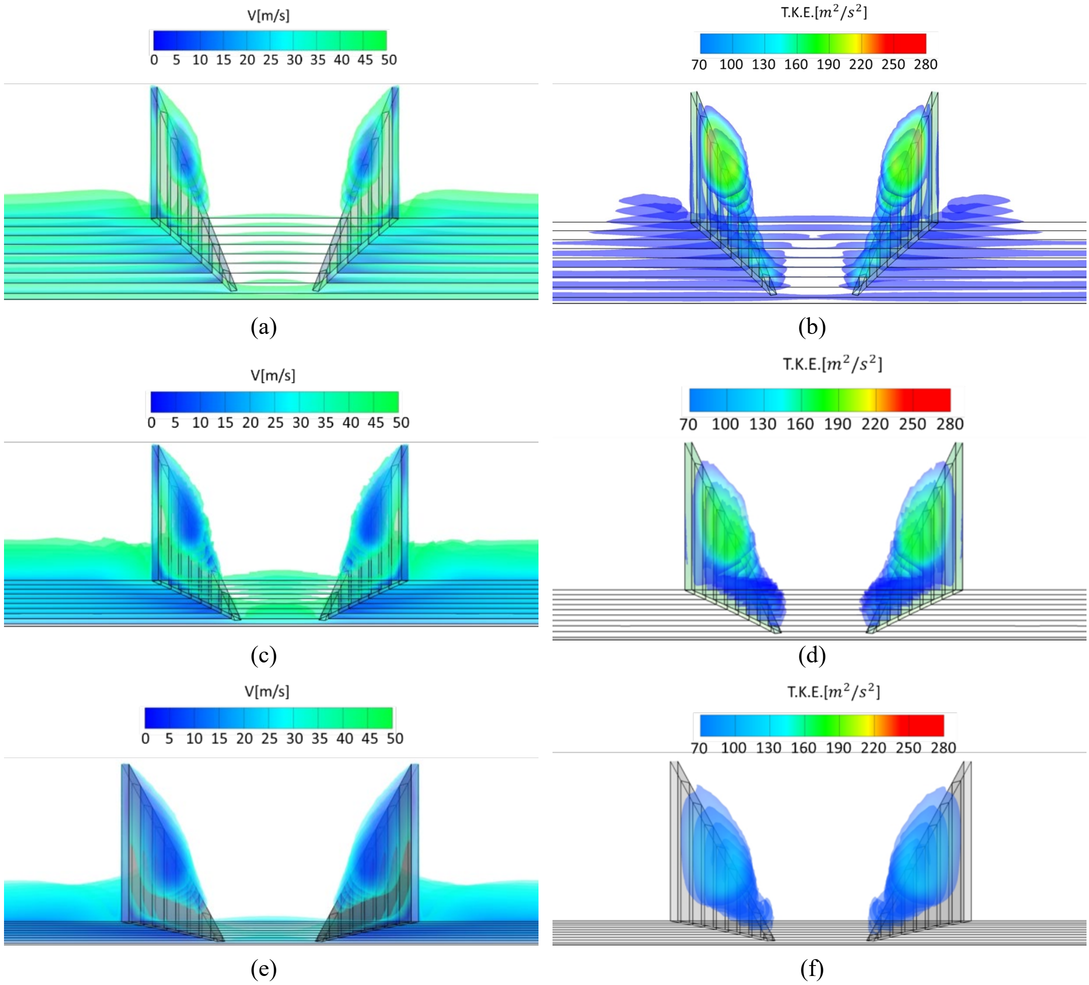

Figure 8. Velocity contours and turbulent kinetic energy contours plotted on equidistant planes for three configurations: C1 [(a),(b)], C2 [(c),(d)], C3 [(e),(f)] at $\alpha = 22^0$

Furthermore, to better understand the highly complex structure of the turbulent flow, on top of the velocity contour representation on equidistant planes, a representation of the streamlines is presented in the figure below. This shows the generation of the vortex tube is happening near the tip of the vortex generator, and as the flow advances, the fluid follows an helicoidal path dictated by the local pressure drop, forming the vortex tube. Moreover, to better comprehend the flow physics related to boundary layer flow, an oil flow visualization was plotted on the surface of the wing. In the middle section of vortex generators, we can see that the flow undergoes a contraction and near the tip of the generator, two large wedges that relates to regions of turbulent flow are starting to form. The mixing process produced by the vortex tubes can be observed after the vortex generators.

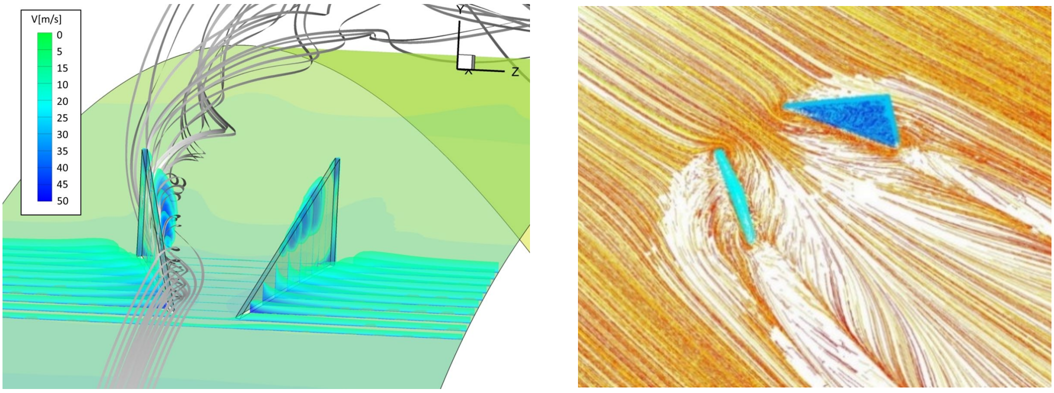

(a) (b)

Figure 9. Streamlines representation (a) and oil flow visualization (b)

Although, velocity and turbulent kinetic energy contours as well as streamline representation or oil flow visualization helps us to better understand the flow physics around the vortex generators, for tridimensional highly turbulent flows, an objective criterion of vortices such as Q criterion could be of help. This criterion is defined as $Q = \frac{1}{2}(\|\Omega\|^2 - \|\mathrm{E}\|^2)$, where Ω represents the vorticity tensor, and E the strain rate tensor. This means that for a region to be defined as a vortex, the fluid rotation must play a leading role in comparison to the strain rate. In the figure below, a visualization using Q criterion is presented, and the creation of the vortex tubes and the highly turbulent flow is clearly shown.

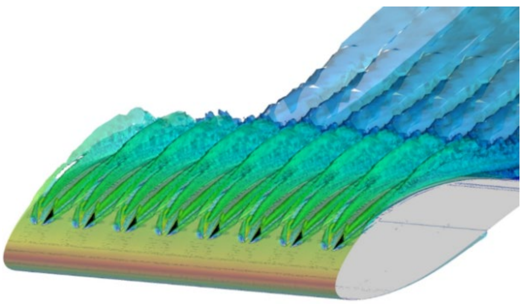

Figure 10. Visualization of the generated vortex tubes on the using Q iso-surface criterion

Numerical simulations have been carried out as part of a parametric study to better understand the flow physics around the vortex generators. Regarding the generator positioning, the parametric study has shown, not only the optimal configuration, but also new validation criteria such as the value of the stall angle, the post stall lift loss, or the area of the recirculation zone. Results have shown that proper positioning of the vortex generators can produce significant improvements in aerodynamic performance for near stall angles of attack.

Comparison between different configurations of vortex generators placements to the base line configurations show, not only increases in lift coefficient, but also a reduction in drag coefficient and an increase in the value of the critical angle of attack. However, the lift curves shows that the post stall lift loss is inversely proportional to the chordwise position of the generators and implies that the efficiency of the control method must consider, not only the lift increment, but also the value of the post stall lift slope for safety reasons. The flow separation zones associated to each configuration shows the beneficial effect of the downstream generated vortex tubes. For proper positionings, the separation occurs only on the lateral sides of the wing section due to energy transport from the outer flow to the boundary layer region in the downstream area of the generators. The pressure coefficient distributions representation on the middle section of the domain for every vortex generator configuration shows that the lift increment is attributed, not only to the vortex tube effect on the downstream flow, but also to the suction effect in the upstream flow region.

The lift increment can be associated with the turbulent mixing process produced by the helicoidally downstream vortices represented with the help of the streamlines. The reduction of the drag coefficient at high angles of attack can be attributed to the highly turbulent flow induced by the generators which contributes to the stall delay. The representation of the velocity contour and the turbulent kinetic energy on equidistant planes perpendicular to the wing section surface contributes to the understanding of the vortex tubes generation. In addition, the oil flow visualization shows that the fluid undergoes a contraction near the tip of the generators with two large wedges of turbulent flow starting to form.

The transport of energy from the outer flow to the boundary layer region can be seen in the downstream flow, not only with the help of the oil flow visualization or streamline representations, but also with the help of iso-surfaces defined by the Q criterion. In addition, the developed automation procedure proved to be robust and can be used to further extend the obtained results with parametric studies of other design variables such as the rotation angle or geometrical parameters. Therefore, the work should be continued, and further numerical studies should be performed not only with different vortex generator geometries but also for different flow regimes.

4. CONCLUSIONS

Numerical simulations have been carried out as part of a parametric study to better understand the flow physics around the vortex generators. Regarding the generator positioning, the parametric study has shown, not only the optimal configuration, but also new validation criteria such as the value of the stall angle, the post stall lift loss, or the area of the recirculation zone. Results have shown that proper positioning of the vortex generators can produce significant improvements in aerodynamic performance for near stall angles of attack.

Comparison between different configurations of vortex generators placements to the base line configurations shows not only increases in lift coefficient, but also a reduction in drag coefficient and an increase in the value of the critical angle of attack. However, the lift curves show that the post stall lift loss is inversely proportional to the chordwise position of the generators and implies that the efficiency of the control method must consider, not only the lift increment, but also the value of the post stall lift slope for safety reasons. The flow separation zones associated to each configuration shows the beneficial effect of the downstream generated vortex tubes. For proper positionings, the separation occurs only on the lateral sides of the wing section due to energy transport from the outer flow to the boundary layer region in the downstream area of the generators. The pressure coefficient distributions representation on the middle section of the domain for every vortex generator configuration shows that the lift increment is attributed, not only to the vortex tube effect on the downstream flow, but also to the suction effect in the upstream flow region.

The lift increment can be associated with the turbulent mixing process produced by the helicoidally downstream vortices represented with the help of the streamlines. The reduction of the drag coefficient at high angles of attack can be attributed to the highly turbulent flow induced by the generators which contributes to the stall delay. The representation of the velocity contour and the turbulent kinetic energy on equidistant planes perpendicular to the wing section surface contributes to the understanding of the vortex tubes generation. In addition, the oil flow visualization shows that the fluid undergoes a contraction near the tip of the generators with two large wedges of turbulent flow starting to form.

The transport of energy from the outer flow to the boundary layer region can be seen in the downstream flow, not only with the help of the oil flow visualization or streamline representations, but also with the help of iso-surfaces defined by the Q criterion. In addition, the developed automation procedure proved to be robust and can be used to further extend the obtained results with parametric studies of other design variables such as the rotation angle or geometrical parameters. Therefore, the work should be continued, and further numerical studies should be performed not only with different vortex generator geometries, but also for different flow regimes.

REFERENCES

[1] I. A. Chaudhry, T. Sultan, F. A. Siddiqui, M. Farhan, and M. Asim, The flow separation delay in the boundary layer by induced vortices, *J Vis (Tokyo)*, vol. **20**, no. 2, pp. 251–261, May 2017, doi: 10.1007/s12650-016-0396-0.

[2] T. K. Barlas and G. A. M. van Kuik, *Review of state of the art in smart rotor control research for wind turbines*, Jan. 2010. doi: 10.1016/j.paerosci.2009.08.002.

[3] J. C. Lin, *Review of research on low-profile vortex generators to control boundary-layer separation*, 2002.

[4] M. B. Bragg and G. M. Gregorek, Experimental study of airfoil performance with vortex generators, *J Aircr*, vol. **24**, no. 5, pp. 305–309, 1987, doi: 10.2514/3.45445.

[5] M. Khoshvaght-Aliabadi, O. Sartipzadeh, and A. Alizadeh, An experimental study on vortex-generator insert with different arrangements of delta-winglets, *Energy*, vol. **82**, pp. 629–639, Mar. 2015, doi: 10.1016/j.energy.2015.01.072.

[6] X. kai Li, W. Liu, T. jun Zhang, P. ming Wang, and X. dong Wang, Analysis of the effect of vortex generator spacing on boundary layer flow separation control, *Applied Sciences (Switzerland)*, vol. **9**, no. 24, Dec. 2019, doi: 10.3390/app9245495.

[7] B. J. Wendt, Parametric study of vortices shed from airfoil vortex generators, *AIAA Journal*, vol. **42**, no. 11, pp. 2185–2195, 2004, doi: 10.2514/1.3672.

[8] H. Mueller-Vahl, G. Pechlivanoglou, C. N. Nayeri, and C. O. Paschereit, Vortex Generators for Wind Turbine Blades: A Combined Wind Tunnel and Wind Turbine Parametric Study, [Online], Available: http://www.asme.org/about-asme/terms-of-use

[9] *Eurodyn 2014 proceedings of the 9th International Conference on Structural Dynamics*, Porto, Portugal, 30 June - 2 July 2014. Authors:International Conference on Structural Dynamics, Álvaro Cunha (Editor), Elsa de Sá Caetano (Editor), P. Ribeiro (Editor), Gerhard Müller (Editor), Print Book, English, 2014, Publisher: Faculty of Engineering], [Porto, 2014.

[10] C. M. Velte and M. O. L. Hansen, Investigation of flow behind vortex generators by stereo particle image velocimetry on a thick airfoil near stall, *Wind Energy*, vol. **16**, no. 5, pp. 775–785, 2013, doi: 10.1002/we.1541.

[11] N. N. Sørensen, F. Zahle, C. Bak, and T. Vronsky, Prediction of the effect of vortex generators on airfoil performance, in *Journal of Physics: Conference Series*, Institute of Physics Publishing, 2014. doi: 10.1088/1742-6596/524/1/012019.

[12] W. Wang, Y. Cao, and T. Okaze, Comparison of hexahedral, tetrahedral and polyhedral cells for reproducing the wind field around an isolated building by LES, *Build Environ*, vol. **195**, May 2021, doi: 10.1016/j.buildenv.2021.107717.

[13] S. Chillon, A. Uriarte-Uriarte, I. Aramendia, P. Martínez-Filgueira, U. Fernandez-Gamiz, and I. Ibarra-Udaeta, JBAY modeling of vane-type vortex generators and study on airfoil aerodynamic performance, *Energies (Basel)*, vol. **13**, no. 10, May 2020, doi: 10.3390/en13102423.

[14] C. Zhu, T. Wang, and J. Wu, Numerical investigation of passive vortex generators on a wind turbine airfoil undergoing pitch oscillations, *Energies (Basel)*, vol. **12**, no. 4, Feb. 2019, doi: 10.3390/en12040654.